Electronic Supplementary Information

for

Dark plasmonic modes based perfect absorption and refractive index sensing

W. H. Yang [a,†], C. Zhang [a,†], S. Sun [a], J. Jing [a], Q. Song [a,b,*] and S Xiao [a,b,*]

a. State Key Laboratory on Tunable laser Technology, Ministry of Industry and Information Technology Key Lab of Micro-Nano Optoelectronic Information System, Shenzhen Graduate School, Harbin Institute of Technology, Shenzhen, China, 518055.

b. Collaborative Innovation Center of Extreme Optics, Shanxi University, Taiyuan 030006 China.

† These authors contribute equally to this research. *Email:shumin.xiao@hit.edu.cn; * Email: qinghai.song@hit.edu.cn

In the main text, we have mentioned many times about the optical properties of metal-covered grating without metallic sidewalls. Here we show the detail information.

1. Numerical simulations of metal-covered PMMA grating without metallic sidewalls.

The cross-section of periodic PMMA grating without sidewalls shown in Fig. S1(a), The thickness of top and bottom silver films are t = 20 nm. The width and height of PMMA strip are w = 110 nm h = 270 nm and p = 290 nm, respectively. By setting the refractive index of PMMA as 1.49 and the permittivity of silver with a Lorentz model, the nanostructure have been numerically studied with COMSOL. Several plasmonic resonances can be excited shown in Fig. S1(b). While some resonances have similar wavelengths to the dark mode in the main text, they still have quite large reflectance and transmittance and are bright. Fig S1(c) and S1(d) show the field pattern (Ey) and normalized field pattern (|E|) of a bright mode at 662 nm. Different from the quadruple mode in the main manuscript, here the electric field is mainly confined around the top silver film and can be considered as dipole (see the arrow in Fig. S1(c))

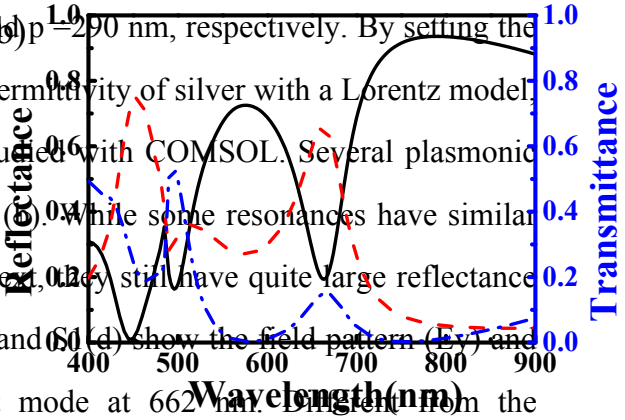

and thus is bright at far field.

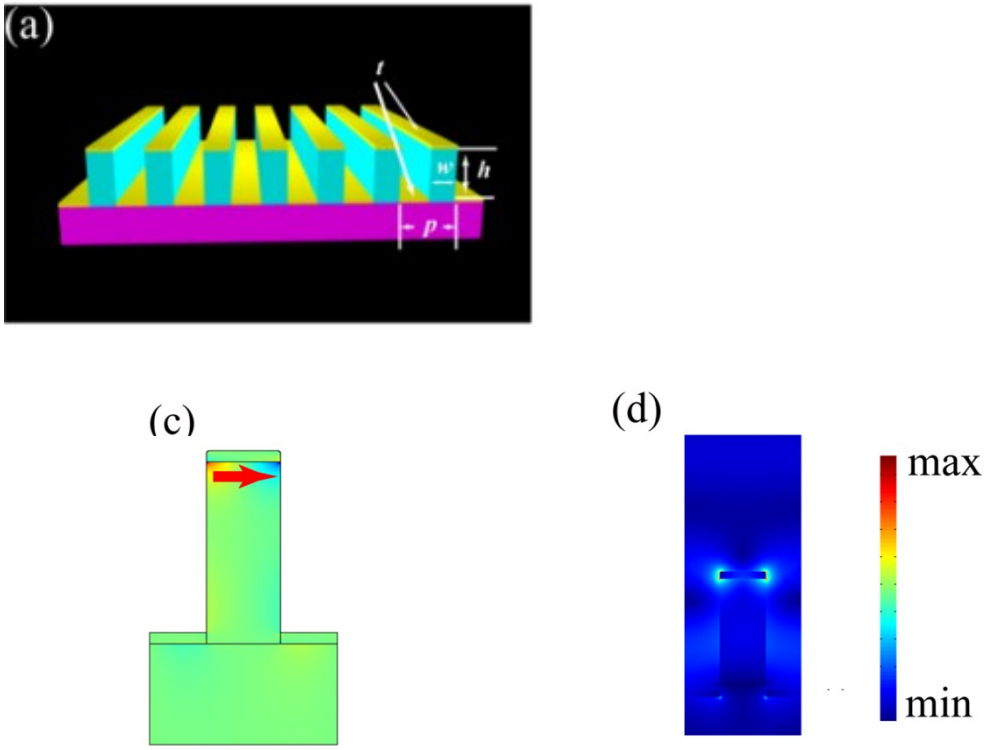

Fig. S1 The numerical results of metal-covered PMMA grating without metallic sidewalls. (a) shows the schematic picture of the nanostructure. (b) The calculated reflection (solid line), transmission (dash-dotted line), and the absorption (dashed line) spectra. (c) shows the field pattern (Ey) of resonant at 662 nm in the cross section of each strip. (d) shows the field pattern (norm E) of resonant at 662 nm in the cross section of each strip.

2. Dark mode in metal-covered PMMA grating with Ag sidewalls

While the metal-covered grating with Ag sidewalls can generate dark modes, there is still one bright mode at 812 nm with obvious reflectance. To understand this resonances, we have numerically calculated the field pattern (E_y) and the normalized field (|E|) in Fig. S2. Although there are still some field distributions along the sidewalls in the vertical directions, we can see that the fields at the bottom silver-substrate interface is much larger than the others. Consequently, the main electromagnetic field distribution can still be analogous to a dipole mode instead of a quadruple mode. Consequently, this resonance is still bright and doesn't have perfect absorption.

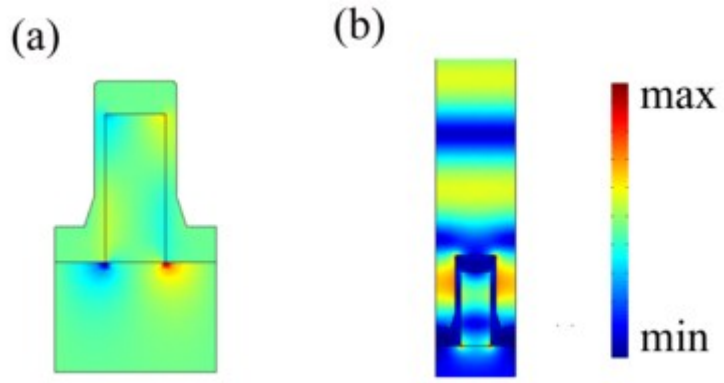

Fig. S2 The numerical results of metal-covered PMMA grating with metallic sidewalls. (a) shows the field pattern (Ey) of resonant at 812 nm in the cross section of each strip. (b) shows the field pattern (norm E) of resonant at 812 nm in the cross section of each strip.

From Fig. S3(a), we can find that the absorption can keep well above 75% with the decrease of t_1 and t_2 ($t_1 = t_2$) from 60 nm to 15 nm. Just like the thickness of the sidewall, this wide range of t_1 and t_2 ensure that a continuous metal can cover on top and bottom of the PMMA grating. However, when the silver thickness of the top (t_1) and bottom (t_2) below the 15 nm, the absorption of the structure changed dramatically. The absorption decreased to below 41% when the thickness of t_1 and t_2 were close to the zero. Meanwhile, we also numerically studied the reflectance spectrum of different t_1 and t_2 ($t_1 = t_2$). As shown in Fig. S3(b), the resonance dips become weaker with the decrease of t_1 and t_2. Similar to the absorption, the drastic change also happened at the 15 nm. When the thickness below the 15nm, the resonance dip almost disappears, indicating that the dark mode is not be generated. These results matched the mechanism proposed before by Gu et al that the top metal of the structure behave like an electric current generator to excite the standing waves within sidewall electrically and form quadruple or higher-order dark modes.

In additional to the thickness of sidewall, we have also studied the dependence of dark modes on the height of sidewalls. By changing the height of PMMA grating, we have numerically calculated the absorption and reflection spectra. All the results are summarized in Fig. S3(c). With the decreases of height from 330 nm to 200 nm, we can see that the absorption (reflection) increases (decreases) first and then decreases (increases). The maximum (minimum) value appears at around 260 nm – 270 nm,

where the resonant wavelengths of standing waves within sidewalls match the resonances of top metal very well.

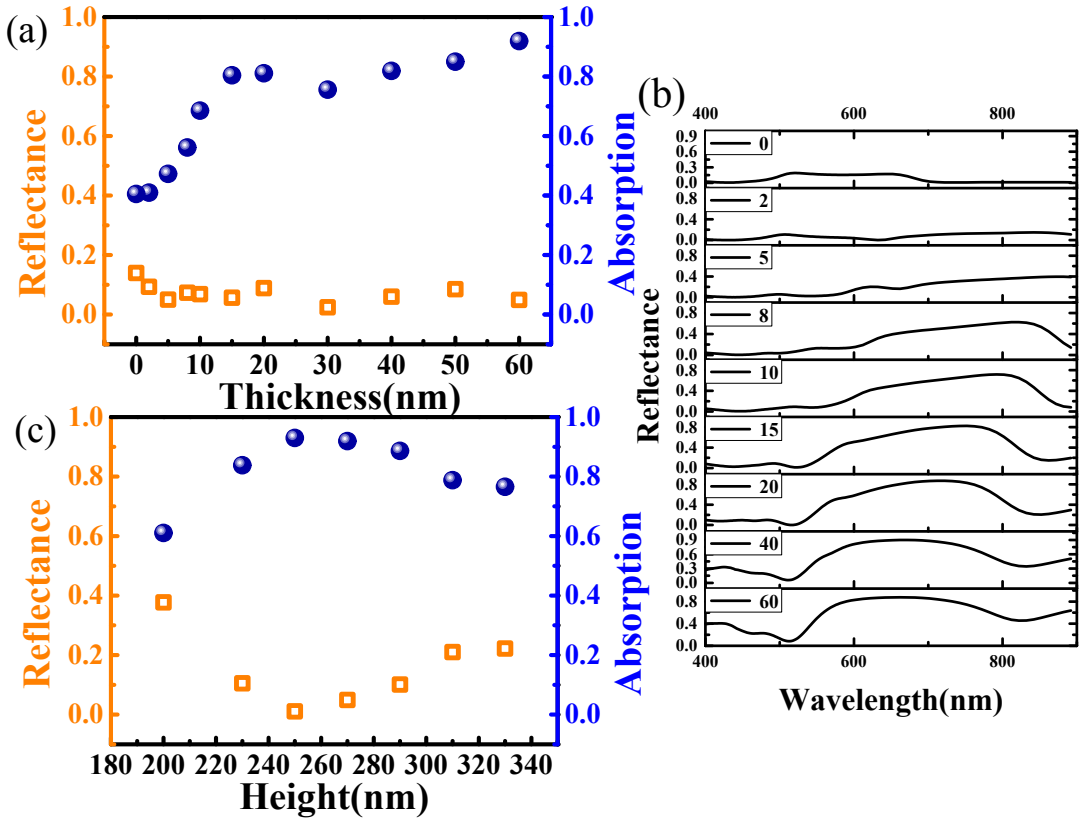

Fig. S3 (a) The reflectance and absorbance of the metal-covered PMMA grating with metallic sidewalls as a function of top (t_1), bottom (t_2) silver thickness, which $t_1 = t_2$ (a) and the height of PMMA. (b) The reflectance of metal-covered PMMA grating with silver sidewalls at different thickness of t_1 and t_2. (c) The reflectance and absorbance of metal-covered PMMA grating with silver sidewalls at different height of PMMA grating.

To further confirm the formation of dark plasmon mode, we have also calculated the resonant spectrum and field patterns of the metallic sidewalls without the top grating. All the other parameters are the same as Fig. 1(c) and the light incidents normally. The results are shown in Fig. S4. Different from Fig. 1(c), here the resonant dip is much broader and shallower. The corresponding field pattern and charge distributions show that the quadruple (dark mode) is hard to optically excited. Therefore, from the differences between Fig. 1(c) and Fig. S4(b) and the corresponding charge distributions, we can conclude that dark plasmon mode has been successfully generated in our designed metallic nanostructures.

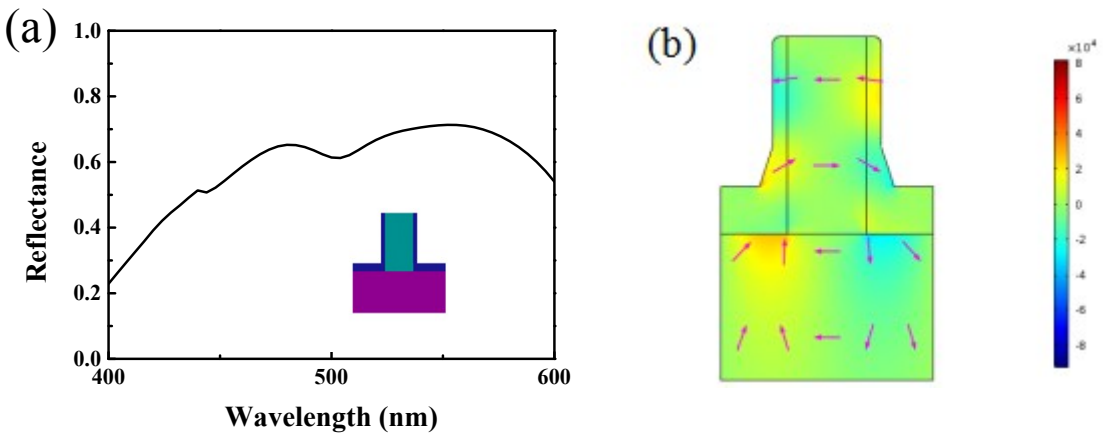

Fig. S4 (a) The reflection spectra of metal-covered PMMA grating without top silver. The inset is the schematic picture of the nanostructure. (b) The field distribution and the charge distribution of the resonant dip in (a) at 488 nm.

3. Fabrication of metal-coated PMMA grating without metallic sidewalls

To experimentally verify the numerical calculations in Fig. S1, we have experimentally fabricated the metal-coated PMMA grating without metallic sidewalls. This kind of structure is very regular in plasmonic research and has been thoroughly studied before. The fabrication procedure is quite similar to the one in main text. It consists of an electron-beam lithography process and a following lift-off. All the fabrication conditions are the same as the main text. The only difference is the last two steps that are used to deposit silver films onto the sidewalls have been neglected. Fig. S5 shows the top-view scanning electron microscope (SEM) image and the side-view SEM image of the fabricated samples. From the top-view SEM, we can still see the periodic gratings. However, the width of each strip is narrower. For a clear view, the silver in Fig. S5(b) are marked with blue color. We can see that both of the top surface and bottoms of grating are well covered silver. However, there is no silver films on the sidewalls. All of these results are very close to the setting in Fig. S1 and can thus be used for the following optical experiments.

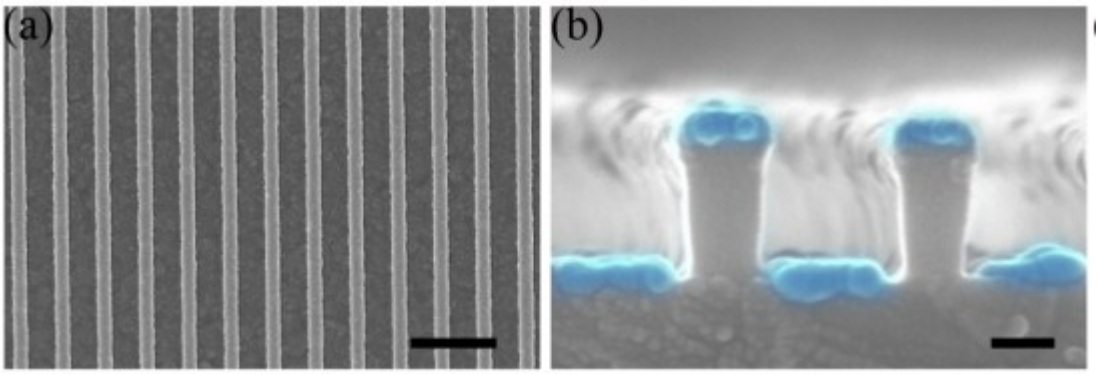

Fig. S5 (a) and (b) are the top-view and side-view SEM images of the metal-covered PMMA grating without silver sidewalls. The scale bar of (a) and (b) are 600 nm, 100 nm, respectively.

4. The setup for optical characterization

In the main manuscript, we have shown the transmission and reflection spectra of metal-covered PMMA grating with silver sidewalls. These spectra are directly measured with the optical setup shown in Fig. S6. Basically, a light beam is collimated by a lens group and its polarization is selected by a Glan prism. Then the light beam is focused onto the sample surface in normal direction with an optical lens (focus length ~ 50 mm). The reflected beam is collected by the same lens and coupled to a spectrometer. Similarly, the transmitted light is collected by another lens and coupled to the spectrometer.

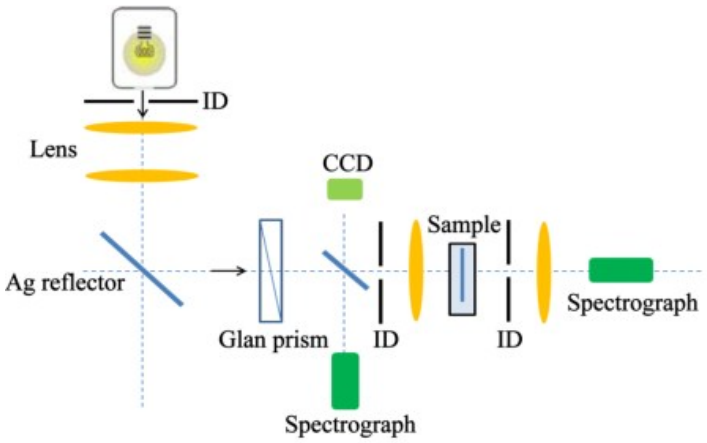

Fig. S6 The optical setup for spectral measurements.

Besides the metal-covered PMMA grating with silver sidewalls, we have also measured the transmission and reflection spectra of the metal-covered PMMA grating

without silver sidewalls for a direct comparison. All the results are shown in Fig. S7. Similar to the numerical calculations, several resonant dips can be seen in the reflection spectrum and the corresponding transmission peaks have also been observed. Consequently, the total absorption of the structure is usually lower than 70% even though the wavelength of incident light is close to the band transition absorption. These results clearly demonstrate the efforts of the silver sidewalls in the formation of dark plasmonic modes.

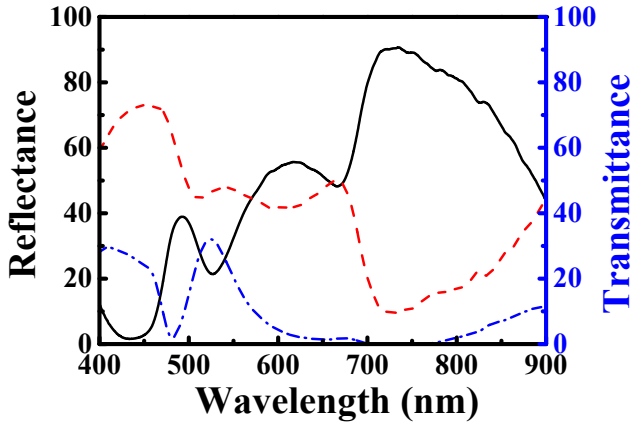

Fig. S7 The experimentally recorded reflection (solid line), transmission (dash-dotted line), and the absorption (dashed line) spectra of metal-covered PMMA grating without metallic sidewalls.

5. The refractive index sensing experiments

As mentioned in the manuscript, the dark plasmonic modes have been applied as refractive index sensors. Here we would like to show the detail experimental results and the corresponding simulations. In our experiments, a glycerin-water mixture was used to change the refractive index. The concentrations of glycerin were chosen to be 0, 10, 18, 26, 34, 42, 50, 57, 64 and 100 wt%, and the corresponding refractive indices were 1.333, 1.345, 1.355, 1.365, 1.376, 1.386, 1.398, 1.409, 1.419, and 1.474,1 respectively. The spectral responses to the refractive index change are shown in Fig. S6. For both of the metal-covered grating with and without silver sidewalls, the resonant dips shifted to longer wavelength with the increase of refractive index.

Figure S8(a) shows the numerically calculated reflection spectra of the metal-covered PMMA grating with metallic sidewalls in glycerin–water mixture solutions at normal incidence under TM-polarization. With the increase of refractive index, we can see

that the resonant dips continuously shift to longer wavelengths. Figure S8(c) summaries the wavelengths as a function of refractive index. We can see that the changes is quite linear and the sensitivity can be fitted as 438 nm/RIU.

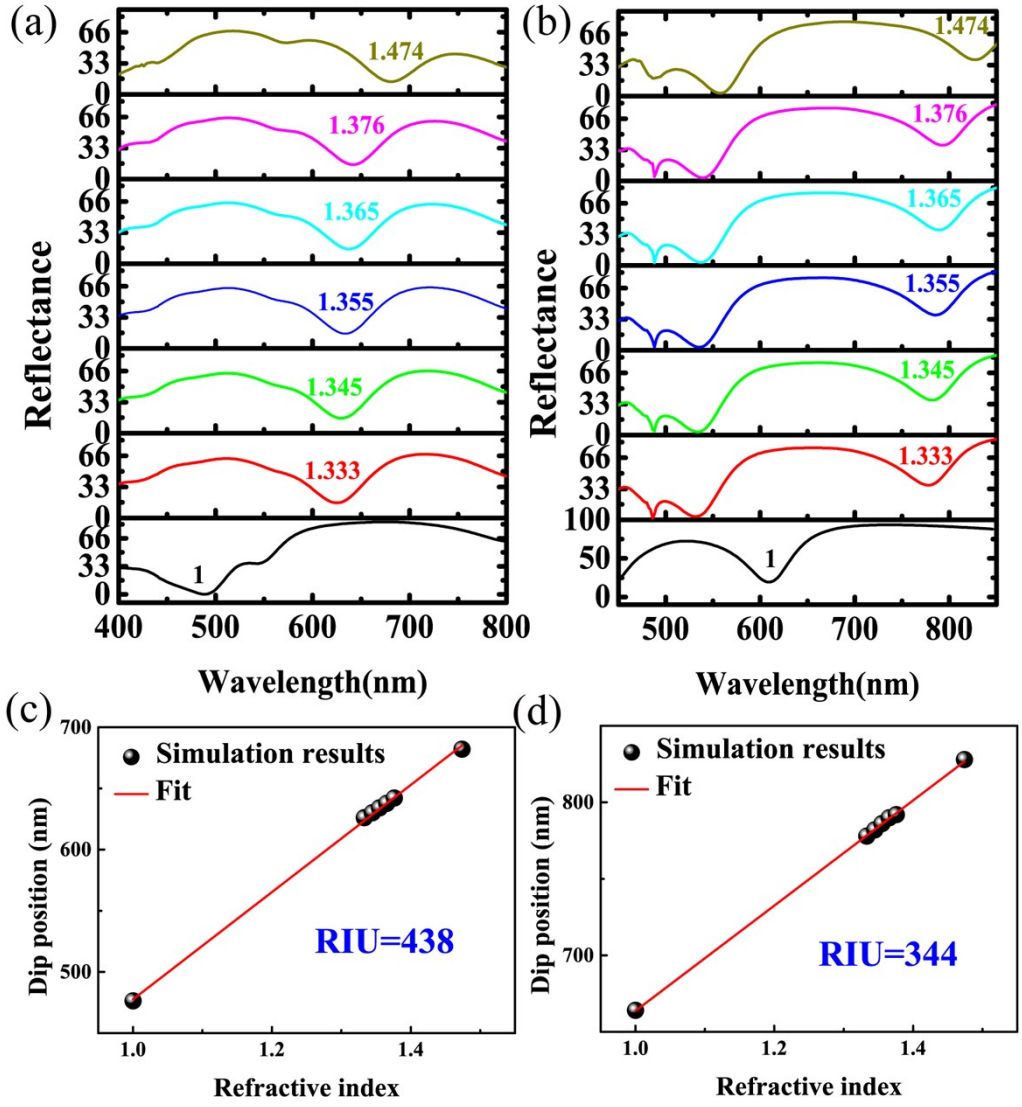

Fig. S8 (a) and (b) are the reflection spectra of numerical results of metal-covered PMMA grating with and without silver sidewalls at different refractive index. (c) and (d) summarize the dependence of resonant wavelengths on the environmental refractive indices.

Similarly, the reflection spectra of metal-covered PMMA grating without silver sidewalls have also been numerically studied. All the results are shown in Fig. S8(c) and Fig. S8(d). Similar to the dark modes in Fig. S8(a), here the resonant dips also shift to longer wavelengths with the increases of refractive index. The only difference is the detection sensitivity is only around 344 nm/RIU, which is almost 100 nm/RIU smaller than the dark modes. In this sense, both of the experimental results and the

numerical simulations confirm that the dark plasmonic modes have potentials in refractive index sensing.

More than the experimentally observed wavelength shifts, we have also done a series of control experiments to exclude the possible damage in the nanostructures during the optical measurements in solutions. After each time of sensing, the samples were washed with DI water three times and blown with compressed air gun gently. Then the samples were mounted on the spectroscopic systems and measured the corresponding reflection spectra. All the results are summarized in Fig. S9. While the reflection spectra changed significantly with the increase of refractive index in Fig. S9(a) and Fig. S9(b), the experimental results in Fig. S9(c), (d) shows that the reflection dips of metal-covered PMMA grating with and without silver sidewalls can be well recovered to their original wavelengths. In this sense, we confirm that the samples were not damaged during the optical experiments and recorded wavelength shifts were caused by the refractive index changes in the surrounding environments.

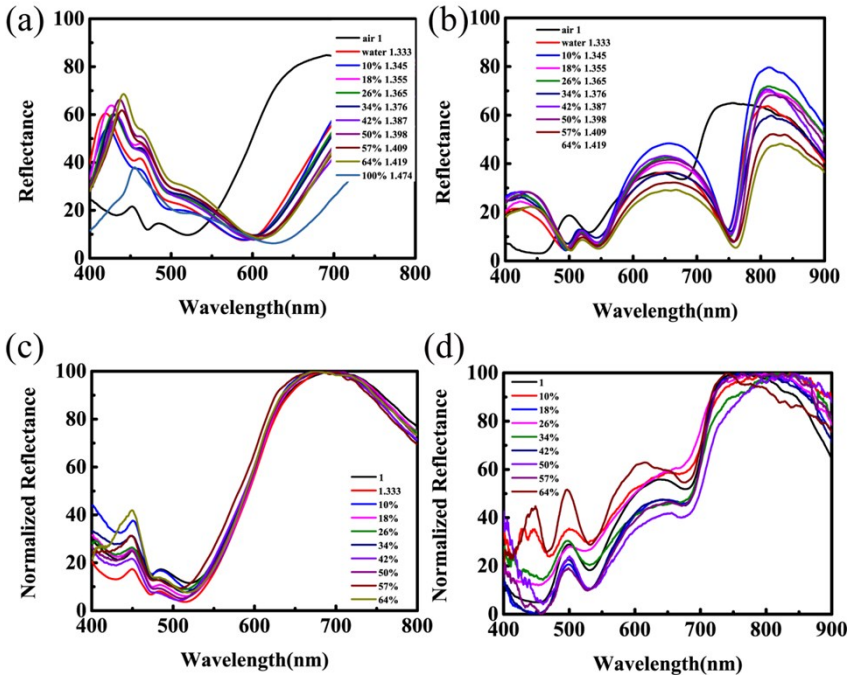

Fig. S9 The experimental results of the second measurement. (a) and (b) are the reflection spectra of metal-covered PMMA grating with and without silver sidewalls at different refractive index. (c) and (d) are the reflection spectra of metal-covered PMMA grating with and without silver sidewalls at different refractive index after washed with distilled water three times.

6. The improvement in figure of merit (FOM)

In principle, the figure of merit (FOM) is an important parameter in applciations such as biosensing. In the main manuscript, we have mainly introduce a simple realization of dark mode with normal incident light. We would like to note that the FOM and the sensitivity can both be improved. Here, we have changed the size parameters to t_1 = 40 nm, t_2 = t_3 =20 nm, h = 250 nm, w = 150 nm and p = 250 nm and numerically simulated the nanostructures. All the results have been summarized and shown in Fig. S10 below.

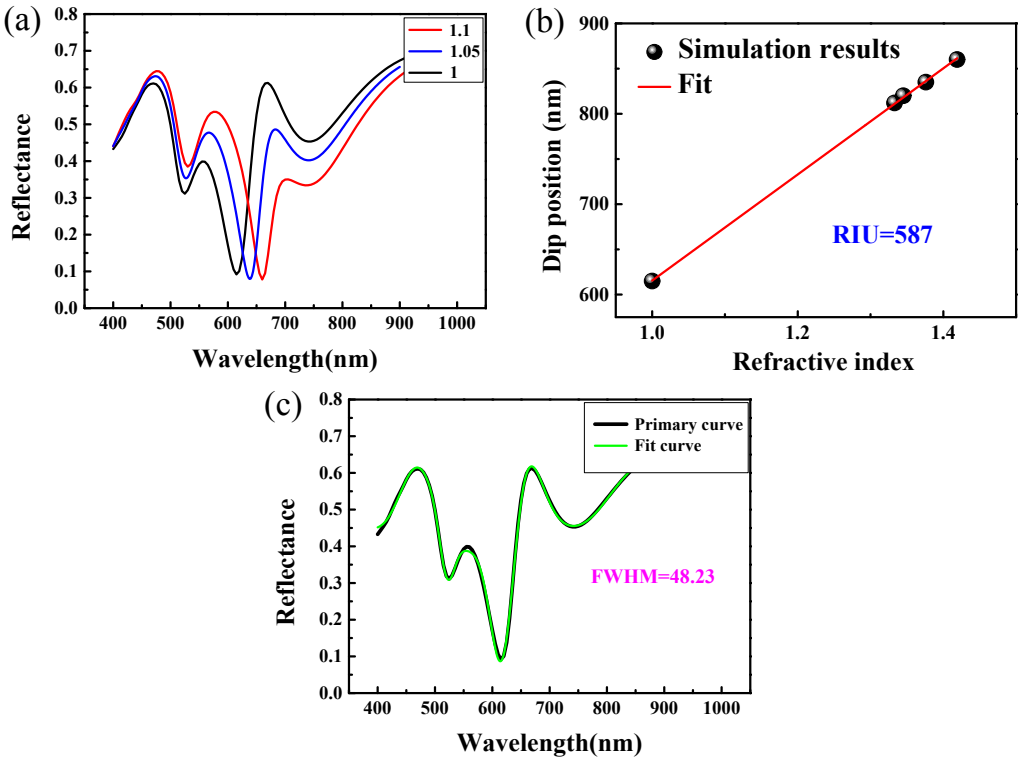

Fig. S10 (a) The simulated reflectance of grating with sidewalls at different refractive index. (b) summarizes the dependence of resonant wavelengths on the environmental refractive indices. (c) The fit curve of the simulated reflectance of grating with sidewalls which the FWHM = 48.23.

Similar to above discussions, here the quadruple (dark plasmon mode) appears at around 610 nm. Fig. S10(a) shows the dependence of the dark mode on the changes in environmental refractive index. A sensitivity around 587/RIU has been successfully achieved. As the linewidth of the dark mode is around 48.23 nm showed in Fig. S10(c), the FOM in this structure can thus be as high as 12.17, which is further

improved. This RIU is pretty high in the existing research at visible range. We believe this study will be used as biosensor which is very helpful.

References

1 Glycerine Producers Association, *Physical properties of glycerine and its solutions*., Glycerine Producers' Association, 1963.